

Impact of strong magnetic field, baryon chemical potential, and medium anisotropy on polarization and spin alignment of hadrons

Bhagyarathi Sahoo,* Captain R. Singh,† and Raghunath Sahoo‡

Department of Physics, Indian Institute of Technology Indore, Simrol, Indore 453552, India

(Dated: February 28, 2024)

The recent observation of global polarization of Λ ($\bar{\Lambda}$) hyperons and spin alignment of ϕ and K^{*0} vector mesons create remarkable interest in investigating the particle polarization in the relativistic fluid produced in heavy-ion collisions at GeV/TeV energies. Among other sources of polarization, the Debye mass of a medium plays a crucial role in particle polarization. Any modification brought to the effective mass due to the temperature, strong magnetic field (eB), baryonic chemical potential (μ_B), and medium anisotropy (ξ), vorticity, etc., certainly affects the particle polarization. In this work, we explore the global hyperon polarization and the spin alignment of vector mesons corresponding to the strong magnetic field, baryonic chemical potential, and medium anisotropy. We find that the degree of polarization is flavor-dependent for hyperons. Meanwhile, vector meson spin alignment depends on the hadronization mechanisms of initially polarized quarks and anti-quarks. Medium anisotropy significantly changes the degree of polarization in comparison with the magnetic field and baryon chemical potential.

I. INTRODUCTION

So far, the thermalized state of strongly interacting partons, called quark-gluon plasma (QGP), is probed in heavy-ion collisions through a baseline, the pp collisions. It was assumed that QGP existence in pp collisions is next to impossible because it lacks the necessary conditions for QGP to be formed. On the contrary, in recent LHC events, ultra-relativistic pp collision experiments have reported behavior similar to heavy-ion collisions, e.g., collective flow, strangeness enhancement, etc [1, 2]. However, other studies suggest similar phenomena may arise due to the other QCD processes [3, 4]. These studies raise a question concerning the present QGP signatures and a need for the next generation of probes. In the quest for such a baseline-independent probe, polarization comes into picture and can have implications for understanding hot QCD matter. The particle production mechanisms lead to a finite polarization of the light/heavy baryons and vector mesons [5]. However, there are various sources by which hadrons can get polarized in ultra-relativistic collisions. One such primary source could be the initial state polarization, which arises due to the motion and spin of the constituent quarks of the colliding nucleons. This initial state polarization can be transmitted to the quarks participating in the collision process. The magnetic field produced by the charged spectator protons in such collisions interacts with the electric charge and spin of the quarks, which may lead to quark polarization. A topological charge imbalance in the presence of an external magnetic field leads to the charge separation in the direction of the magnetic field. This phenomenon

is known as the chiral magnetic effect (CME) [6, 7]. If QGP exhibits chiral symmetry restoration, then CME could lead to quark polarization along the direction of the magnetic field. A similar phenomenon called chiral vortical effect (CVE) is expected due to the non-zero local vorticity, which also contributes to the hadron polarization [8, 9]. The hydrodynamic behavior or collective motion of QGP can also induce polarization in the quark distribution due to the anisotropic expansion [10, 11]. Determining the precise sources and types of polarization in ultra-relativistic collisions requires sophisticated theoretical studies with corresponding experimental observations.

In 2005, Liang and Wang predicted in non-central heavy-ion collisions, the orbital angular momentum (OAM) of the partonic system polarizes the quarks and anti-quarks through spin-orbit coupling. They asserted that the initial partons created in the collisions could generate a longitudinal fluid shear distribution representing the local relative OAM in the same direction as global OAM at a finite impact parameter. This quark polarization manifests the polarization of the hadrons (with finite spin) along the direction of OAM during the process of hadronization [12–15]. Apart from global polarization of hadrons, such global quark polarization has many observable consequences, such as left-right asymmetry in hadron spectra and global transverse polarization of thermal photons, dileptons, etc. [16, 17]. They have studied the global polarization of hyperons [12] and spin alignment of vector mesons [13] in different hadronization scenarios. Following, in 2013, Becattini et al. predicted the global spin polarization of Λ hyperons due to the OAM-manifested thermal vorticity [18]. Various theoretical predictions of global Λ hyperons polarization by different hydrodynamic and transport models are well agreed with the experimental results available at Relativistic Heavy Ion Collider (RHIC) [19–27]. These hydrodynamic and transport

* Bhagyarathi.Sahoo@cern.ch

† captainriturajsingh@gmail.com

‡ Raghunath.Sahoo@cern.ch (Corresponding Author)

models considered the thermal equilibrated distribution of spin degrees of freedom for polarization studies [28–35].

In addition to Λ hyperons, the averaged global polarization measurement of Ω and Ξ hyperons are obtained using the polarization transfer method in STAR [36]. Similarly, the polarization of quarkonium states is obtained by measuring the angular distribution of dileptons [5, 37–40]. Furthermore, the global spin alignment of ϕ , K^{*0} , K_S^0 mesons is observed at the LHC and RHIC from the angular distribution of decay daughters in the mother particles’s rest frame [41–46]. Recent spin alignment measurements for ϕ vector mesons by the STAR collaboration initiate a spark in the theoretical communities to investigate the source of large positive spin alignment for ϕ vector meson, while K^{*0} shows no such spin-alignment within uncertainties [41].

Some theoretical studies claim that in addition to vorticity and electromagnetic fields, a strong vector meson force field is responsible for hyperon polarization [47] as well as spin alignment of vector mesons [48, 49]. Recently, Sheng et al. [49] explain the large spin alignment of ϕ vector meson in a quark polarization mechanism by a strong force field, in which quarks interact with the dense medium through a strong force and become polarized. The strong force field is proposed to polarize the vector meson with the hidden flavor quantum number. Apart from these sources, there could be various other possible sources for vector meson spin-alignment, which need further investigation. Moreover, recent observation of longitudinal local polarization of Λ hyperons at LHC and RHIC mismatches with the theoretical predictions [11], which opens a new door for the heavy-ion community to have intense investigations on this topic. However, various studies have been developed to solve this puzzle through different aspects [50, 51]. Similar to hyperons, the local polarization of quarks and anti-quarks due to anisotropic expansion of the medium contributes to the spin alignment of vector meson [52]. The authors have argued that the deviation of ρ_{00} from 1/3 is not solely coming from global spin alignment but also has the contribution of quarks and/or anti-quarks, which are locally polarized. However, the contribution of local quark polarization requires the measurement of off-diagonal elements of the spin density matrix.

In the experiment, the methods used to measure polarization for hyperons and vector mesons are different. However, both depend on the angular distribution of decay daughters in the mother particles’ rest frame. The hyperons undergo parity-violating weak decays, while the vector mesons mainly decay through the parity, conserving strong decay. The Λ hyperon polarization is estimated by the projection of the daughter proton’s momentum along the OAM (or vorticity axis) direction. On the other hand, the spin alignment of vector meson has been studied by measuring the ρ_{00} element of the

spin density matrix. The detailed explanation of the spin density matrix is discussed in section II.

Ultra-peripheral heavy-ion collisions have several consequences; one such example is that they produce a strong magnetic field. This magnetic field decays with time and can, in principle, affect the QGP medium evolution, thermodynamic, and transport properties [53–55]. The magnetic field is believed to affect the Λ polarization, specifically on the polarization splitting of Λ and $\bar{\Lambda}$ at the lower center of mass energies. The effect of magnetic field on polarization and spin alignment of hadrons is discussed in Ref. [56–64]. Recent observation of global polarization of Λ hyperons indicate that hyperon polarization decreases with the increasing center of mass energy [19–21]. So, at lower energies, the probability of particles getting polarized is large, which could be a consequence of baryon stopping. This high baryon chemical potential may affect the evolution process and particle polarization. Further, due to the rapid longitudinal expansion of the fireball created in heavy-ion collisions, a high degree of momentum-space anisotropy is produced in the QGP medium in its local rest frame [65]. This momentum-space anisotropy has many novel consequences; for example, it is essential in modeling heavy-quark dynamics, making the inter-quark potentials spatially anisotropic. This anisotropy in the QGP medium may affect the particle yield, flow coefficients, particle polarization, etc.

In this work, we investigate the effect of static strong magnetic field, baryon chemical potential, and momentum-space anisotropy parameter on the polarization of hyperons and spin alignment of vector mesons through Debye screening mass. Please note that in the rest of the paper, we shall refer to Debye screening mass as Debye mass. The individual and combined effect of eB , μ_B and ξ on the polarization and spin-alignment of hadrons is studied. It is important to mention that the magnetic field may generate an additional anisotropy in the medium, which is not explicitly considered in this study. We consider two different hadronization mechanisms, i.e., the recombination and fragmentation processes, for both hyperons and vector mesons.

The structure of this work is as follows. The section II gives a detailed overview of the formalism used in this work. We briefly examine the results in section III and provide a summary in section IV

II. FORMULATION

The global quark polarization is obtained through parton elastic scattering within the framework of an effective static potential model. This model uses effective mass or Debye mass to incorporate the parton scattering, which induces the quark polarization [12–15], given as,

$$P_q = -\frac{\pi}{2} \frac{m_D p}{E(E + m_q)} \quad (1)$$

where $E = \sqrt{p^2 + m^2}$, p and m_q are the energy, momentum, and mass of quark in the center of mass frame of the parton scattering, m_D is the Debye mass.

Assuming $P_u = P_d \equiv P_q$, recent studies [56] calculated the polarization of hyperons using a spin density matrix. The following study is consistent with the previous findings [12], where the authors have calculated the polarization of hyperons using recombination and fragmentation processes.

This global quark polarization leads to the global hyperons polarization at the hadronization stage. The global polarization due to exclusive recombination process for Λ , Σ^\pm , Ξ^- , Ω^- , and Δ^{++} hyperons are given as [12, 56];

$$P_\Lambda^{rec} = P_s, \quad P_{\Sigma^\pm}^{rec} = \frac{4P_q - P_s - 3P_s P_q^2}{3 - 4P_q P_s + P_q^2} \quad (2)$$

$$P_{\Xi^-}^{rec} = \frac{4P_s - P_q - 3P_q P_s^2}{3 - 4P_q P_s + P_s^2}, \quad P_{\Omega^-}^{rec} = \frac{P_s(5 + P_s^2)}{1 + P_s^2} \quad (3)$$

$$P_{\Delta^{++}}^{rec} = \frac{P_u(5 + P_u^2)}{1 + P_u^2} \quad (4)$$

The hyperon polarization from inclusive recombination is difficult to estimate. However, at the extreme limit of inclusive recombination (i.e., fragmentation), the hyperon polarization due to polarized quarks is estimated in Ref. [12]. The fragmentation of hyperons is given by;

$$P_\Lambda^{frag} = \frac{n_s P_s}{n_s + 2f_s}, \quad P_{\Sigma^\pm}^{frag} = \frac{4f_s P_q - n_s P_s}{3(n_s + 2f_s)} \quad (5)$$

$$P_{\Xi^-}^{frag} = \frac{4n_s P_s - f_s P_q}{3(2n_s + f_s)}, \quad P_{\Omega^-}^{frag} = \frac{P_s}{3}, \quad P_{\Delta^{++}}^{frag} = \frac{P_u}{3} \quad (6)$$

Such global polarization of quarks and anti-quarks also describes the spin alignment of vector mesons through different hadronization scenarios [13].

Unlike spin-polarization for hyperons, the spin alignment of vector meson is described by the spin density matrix $\rho_{m,m'}$, where m and m' label the spin component along the quantization axis. The spin alignment for vector meson is mostly measured by the 00^{th} element of the spin density matrix, i.e., ρ_{00} . It can be measured experimentally through the angular distribution of the decay products of the particles rest frame [43]. The deviation of ρ_{00} from $1/3$ (i.e. $\rho_{00} - 1/3$) determines

the degree of alignment of vector meson. In Ref. [13], the authors have described the spin alignment of vector mesons in different hadronization scenarios.

In this work, we consider two scenarios of the hadronization process; the first one is due to the recombination of polarized quarks and anti-quarks. The second one is due to the recombination of polarized quarks and anti-quarks, in which either of them is created in the fragmentation process. The 00^{th} element of spin density matrix for ρ , ϕ and K^* mesons in recombination and fragmentation processes in which both quarks and anti-quarks are polarized are obtained as,

$$\rho_{00}^{\rho(rec)} = \frac{1 - P_q^2}{3 + P_q^2}, \quad \rho_{00}^{\phi(rec)} = \frac{1 - P_s^2}{3 + P_s^2}, \quad \rho_{00}^{K^*(rec)} = \frac{1 - P_q P_s}{3 + P_q P_s} \quad (7)$$

$$\rho_{00}^{\rho(frag)} = \frac{1 + \beta P_q^2}{3 - \beta P_q^2}, \quad \rho_{00}^{\phi(frag)} = \frac{1 + \beta P_s^2}{3 - \beta P_s^2} \quad (8)$$

$$\rho_{00}^{K^*(frag)} = \frac{f_s}{n_s + f_s} \frac{1 + \beta P_q^2}{3 - \beta P_q^2} + \frac{n_s}{n_s + f_s} \frac{1 + \beta P_s^2}{3 - \beta P_s^2} \quad (9)$$

where $\beta \simeq 0.5$. n_s and f_s are the strange quark abundances relative to up and down quarks in QGP and quark fragmentation, respectively.

Further, we have briefly outlined the formalism to explore the effect of magnetic field, baryon chemical potential, and anisotropic parameters on the polarization of hyperons and mesons.

A. Debye Mass under Strong Magnetic Field

The magnetic field produced in the peripheral heavy-ion collisions is believed to decay very quickly. So, it is expected to only affect the partonic phase during the early stage of the evolution process. Magnetic fields tend to align charged particles in a specific direction, resulting in the polarization of the system. Given that quarks possess a fractional electric charge, it is anticipated that a magnetic field could potentially modify the orientation of quarks within the QGP phase. Consequently, in the presence of a strong magnetic field, the total Debye mass for fermions or quarks in the static limit has been calculated through the temporal component of one loop vacuum self-energy diagram and has the following form [66–69];

$$m_D^2(T, eB) = 4\pi\alpha_s(\Lambda^2, |eB|) \left[T^2 \frac{N_c}{3} + \sum_f \frac{|q_f eB|}{4\pi^2} \right] \quad (10)$$

here, $\alpha_s(\Lambda^2, |eB|)$ is the running coupling constant, which depends on the magnetic field and temperature. It can be written as [68],

$$\alpha_s(\Lambda^2, |eB|) = \frac{g_s^2}{4\pi} = \frac{\alpha_s(\Lambda^2)}{1 + b_1 \alpha_s(\Lambda^2) \ln \left(\frac{\Lambda^2}{\Lambda^2 + |eB|} \right)} \quad (11)$$

with

$$\alpha_s(\Lambda^2) = \frac{1}{b_1 \ln \left(\frac{\Lambda^2}{\Lambda_{MS}^2} \right)} \quad (12)$$

where $b_1 = \frac{11N_c - 2N_f}{12\pi}$, $\Lambda_{MS} = 0.176$ GeV for $N_f = 3$ and renormalization scale $\Lambda = 2\pi T$ [70].

B. Debye Mass with Baryon Chemical Potential

Finite μ_B dictates the dominance of the number of quarks over anti-quarks, such an imbalance affects the final production yield of hadrons. In nature, any order parameter or disparity ultimately leads to the polarization of the system. Likewise, a non-zero baryon chemical potential can be the source of a polarized QGP medium. Any change brought to the QGP affects its effective mass, as a consequence, μ_B is incorporated in the Debye mass. In a hot and high baryon density medium ($T, \mu_B \gg m_q$, with m_q as the light quark mass), the leading order HTL/HDL calculation predicts resultant Debye mass which has the following form [71–74];

$$m_D^2(T, \mu_B) = 4\pi\alpha_s(\Lambda^2) \left[T^2 \left(\frac{N_c}{3} + \frac{N_f}{6} \right) + \sum_f \frac{\mu_B^2}{18\pi^2} \right] \quad (13)$$

Here, the strong coupling constant $\alpha_s(\Lambda^2)$ takes the form given in Eq. 12, and in the presence of baryon chemical

potential, the renormalization scale is modified into

$$\Lambda = 2\pi \sqrt{T^2 + \frac{\mu_B^2}{\pi^2}} \quad (14)$$

C. Effect of Anisotropy on Debye Mass

Momentum space anisotropy originated due to the collision geometry causing differential expansions of the fireball along the longitudinal and transverse directions. As a consequence, it also alters the effective mass of the medium. The effect of momentum-space anisotropy of the medium on Debye mass is given as [65, 75–79];

$$m_D(T, \xi) = m_D(T) \left[f_1(\xi) \cos^2 \theta + f_2(\xi) \right]^{-\frac{1}{4}} \quad (15)$$

and,

$$m_D(T) = \sqrt{4\pi\alpha_s(\Lambda^2)T^2 \left(\frac{N_c}{3} + \frac{N_f}{6} \right)} \quad (16)$$

The parameter ξ measures the degree of momentum-space anisotropy, defined as;

$$\xi = \frac{1 \langle \mathbf{k}_\perp^2 \rangle}{2 \langle k_z^2 \rangle} - 1 \quad (17)$$

where $k_z \equiv \mathbf{k} \cdot \mathbf{n}$, $\mathbf{k}_\perp \equiv \mathbf{k} - \mathbf{n}(\mathbf{k} \cdot \mathbf{n})$ correspond to the particle momenta along and perpendicular to the direction of anisotropy, and θ is the angle between quark pair alignment (\mathbf{r}) with respect to direction of anisotropy (\mathbf{n}). The $f_1(\xi)$ and $f_2(\xi)$ are parameterized in such a way that Eq. 15 remains always true under small and large values of ξ ,

$$f_1(\xi) = \frac{9\xi(1+\xi)^{\frac{3}{2}}}{2\sqrt{3+\xi}(3+\xi^2)} \frac{\pi^2(\sqrt{2} - (1+\xi)^{\frac{1}{8}}) + 16(\sqrt{3+\xi} - \sqrt{2})}{(\sqrt{6} - \sqrt{3})\pi^2 - 16(\sqrt{6} - 3)} \quad (18)$$

$$f_2(\xi) = \xi \left(\frac{16}{\pi^2} - \frac{\sqrt{2}(\frac{16}{\pi^2} - 1) + (1+\xi)^{\frac{1}{8}}}{\sqrt{3+\xi}} \right) \left(1 - \frac{(1+\xi)^{\frac{3}{2}}}{1 + \frac{\xi^2}{3}} \right) + f_1(\xi) + 1 \quad (19)$$

D. Net Debye Mass

In previous sections, we have discussed the Debye mass for individual cases now combining all together (eB , μ_B , and ξ), we have obtained the resultant Debye mass;

$$m_D(T, \mu_B, B, \xi) = m_D(T, \mu_B, B) \left[f_1(\xi) \cos^2 \theta + f_2(\xi) \right]^{-\frac{1}{4}} \quad (20)$$

and

$$m_D(T, \mu_B, B) = \sqrt{4\pi\alpha_s(\Lambda^2, |eB|) \left[T^2 \frac{N_c}{3} + \sum_f \frac{|q_f eB|}{4\pi^2 T} \int_0^\infty dp_z \{n^+(E)(1 - n^+(E)) + n^-(E)(1 - n^-(E))\} \right]} \quad (21)$$

with

$$n^\pm(E) = \left[\exp \left(\frac{E \mp \mu_B}{T} \right) + 1 \right]^{-1} \quad (22)$$

The $n^+(E)$ and $n^-(E)$ are the phase-space distribution functions of quarks and anti-quarks, respectively.

III. RESULTS AND DISCUSSION

Following the discussed formulation, we studied the influence of magnetic field (eB), baryon chemical potential (μ_B), and anisotropic parameter (ξ) on the polarization of hyperons and spin alignment of vector mesons. As quark-antiquark polarization leads to global hadron polarization, based on that, we have predicted the global polarization of various hadrons. Further, The spin alignment of vector mesons and polarization of hyperons are obtained corresponding to two different hadronization processes: (i) recombination and (ii) fragmentation. Firstly, the hyperon polarization prediction is given and discussed. Subsequently, the spin-alignment of vector mesons is presented. But before that, the change in the Debye mass due to magnetic field, baryon chemical potential, and the anisotropic parameter is depicted in Fig 1 to ensure the validity of our results. It shows the variation of effective Debye mass with the magnetic field (left panel), baryon chemical potential (middle panel), and anisotropic parameter (right panel) for three different values of temperature, i.e., $T = 200$ MeV, $T = 250$ MeV, and $T = 300$ MeV.

The left panel of Fig. 1 shows that the Debye mass increases with magnetic field and temperature. However, the impact of the external magnetic field on the rate of change in Debye mass is stronger at lower temperatures. The observed enhancement in the Debye mass with the external magnetic field is in qualitative agreement with the findings reported in Refs. [80–82]. The middle panel of Fig. 1 reveals a modest decrease in the Debye mass with increasing baryon chemical potential in a baryon-rich medium. Although its decrease is very small in magnitude, the effect of baryon chemical potential is a bit prominent at lower temperatures compared to higher temperatures. In the right panel of Fig. 1, we found that the Debye mass decreases significantly as the anisotropy parameter increases. The decrease in the Debye mass with the momentum anisotropy agrees well with the finding reported in Refs. [65, 75].

Based on these observations, it can be said that the medium effects are encoded in the Debye mass. It is

more sensitive to the anisotropy parameter than the magnetic field and baryon chemical potential. The Debye mass of the medium represents the change in the degree of freedom of the systems, if the Debye mass of the system is very small, then the color degrees of freedom would reduce to the hadron degree of freedom. The Debye mass depends on two things: the medium's temperature (energy) and the coupling strength of the medium. The magnetic field in the medium gives an additional boost to the energy level and strengthens the coupling constant. Due to this, a positive change in Debye mass with increasing field can be seen in the left panel of Fig. 1. On the other hand, finite baryon chemical potential also provides additional energy to the medium but reduces the coupling strengths. Consequently, in Fig. 1, we observe the negative change in the Debye mass with increasing baryon chemical potential. Meanwhile, the anisotropy of the medium does not affect the coupling strength of the medium. However, an uneven distribution of the partons in the medium measured in terms of ξ reduces the net effective mass of the medium. Therefore, a visible reduction in the Debye mass with large values of ξ is observed in Fig. 1. The combined effect of the magnetic field, baryon chemical potential, and medium anisotropy on Debye mass can be estimated using Eq. 21, which is not explicitly illustrated in this work. But one can easily infer the combined effect of these parameters on Debye mass from Fig. 1.

Furthermore, it is noteworthy to mention that in the quark recombination model, the hyperon polarization and spin alignment of vector meson from polarized quarks and anti-quarks does not include momentum dependence explicitly. This momentum dependence is introduced in a non-relativistic quark-coalescence model through the spin-density matrix [56], with which the polarization of vector meson and baryon of spin-1/2 and spin-3/2 is calculated systematically. However, the conventional quark coalescence or recombination models do not include the spin degrees of freedom. Again, the quark coalescence model is improved in Ref. [57].

A. Polarization of hyperons

To understand the polarization dynamics of hyperons, it is crucial to understand how these polarized quarks recombine to produce the final polarized hyperons. The polarization of hyperons depends on the process of hadronization. Here, we estimate the individual and combined effect of magnetic field, baryon chemical potential, and medium anisotropy on the global polar-

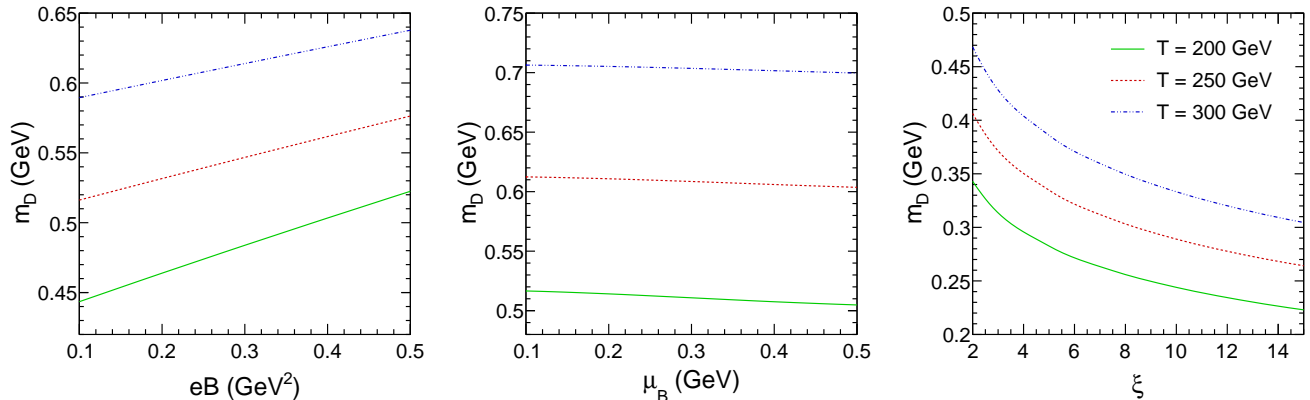


FIG. 1: (Color online) The variation of Debye screening mass (m_D) as a function of magnetic field (eB)(left panel), baryon chemical potential (μ_B)(middle panel) and anisotropic parameter (ξ)(right panel) for three different values of temperatures, i.e $T = 200$ MeV, $T=250$ MeV, and $T = 300$ MeV.

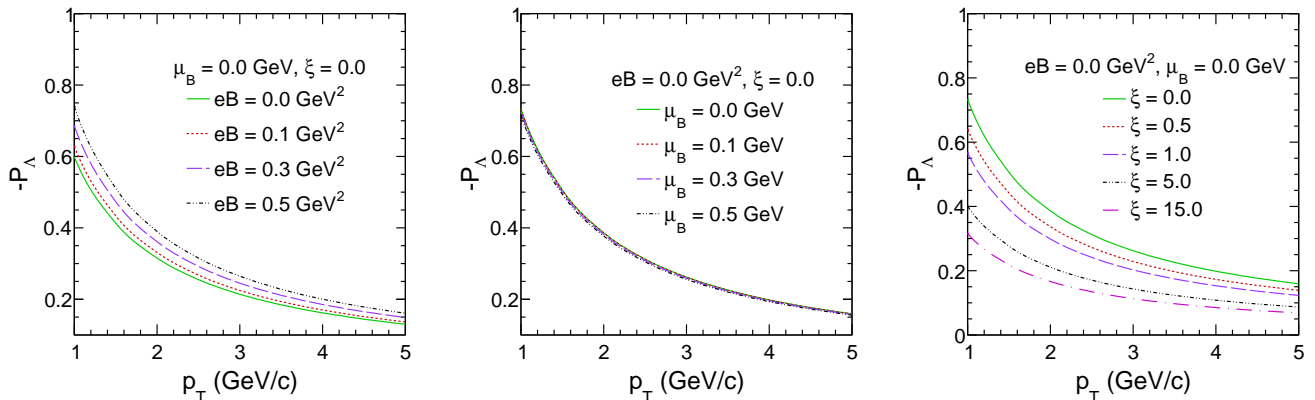


FIG. 2: (Color online) The variation of Λ hyperon polarization as a function of transverse momentum due to recombination process in the presence of magnetic field (eB)(left panel), baryon chemical potential (μ_B)(middle panel) and anisotropic parameter (ξ)(right panel) at temperature $T = 200$ MeV.

ization of hyperons.

The polarization of Λ , Σ^\pm , Ξ^- , Δ^{++} , and Ω^- hyperons in quark recombination process is calculated using the Eqs. 2, 3, 4. The left panel of Fig. 2 shows the variation of Λ hyperon polarization as a function of the transverse momentum (p_T) for different values of the magnetic field at $\mu_B = 0$ GeV and $\xi = 0$ in recombination process of hadronization. We consider three finite values of the magnetic field, i.e., $eB = 0.1, 0.3, \text{ and } 0.5$ GeV². Figure 2 indicates the polarization of Λ hyperon decreases as a function of the p_T for all values of the magnetic field. It is observed that the increase in polarization of the Λ hyperon with a magnetic field can be attributed to the corresponding increase in the Debye mass. Apart from that, the magnetic field helps

to polarize the particle and anti-particle through their magnetic moments. The Λ hyperon has a negative magnetic moment, whereas the $\bar{\Lambda}$ hyperon has a positive magnetic moment. In the presence of a magnetic field, the spin of the $\bar{\Lambda}$ is strongly aligned along the direction of the field, while the Λ spin is relatively poorly aligned against the direction of the field. This argument could qualitatively describe the splitting of Λ and $\bar{\Lambda}$ hyperon with $P_{\bar{\Lambda}} > P_\Lambda$. However, current formalism predicts the same polarization for Λ and $\bar{\Lambda}$. Moreover, various phenomenological studies suggest that hyperon polarization is directly proportional to the magnetic field and plays a crucial role in particle polarization [56, 58].

During the exclusive recombination process of hadronization, it has been observed that the polarization

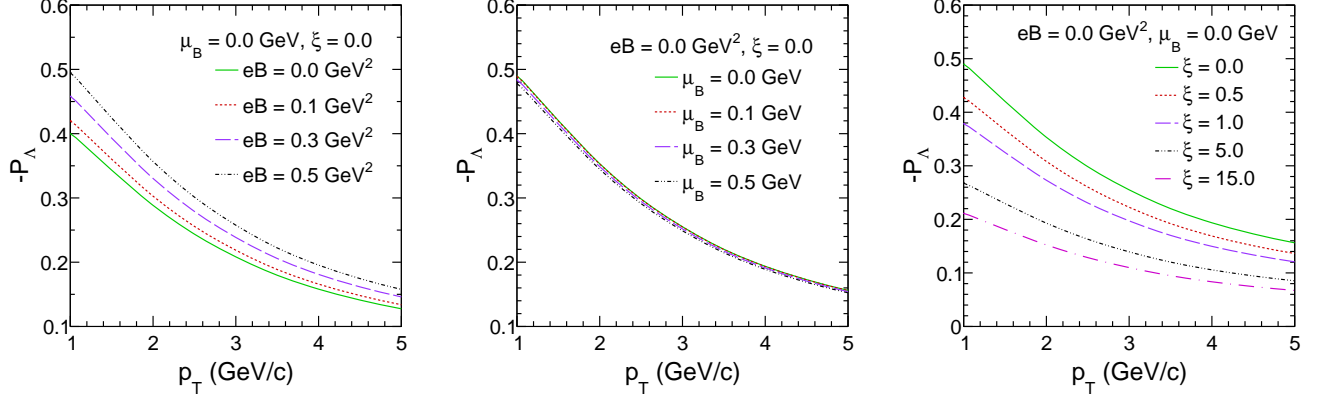


FIG. 3: (Color online) The variation of Λ hyperon polarization as a function of transverse momentum due to fragmentation process in the presence of magnetic field (eB)(left panel), baryon chemical potential (μ_B)(middle panel) and anisotropic parameter (ξ)(right panel) at temperature $T = 200$ MeV.

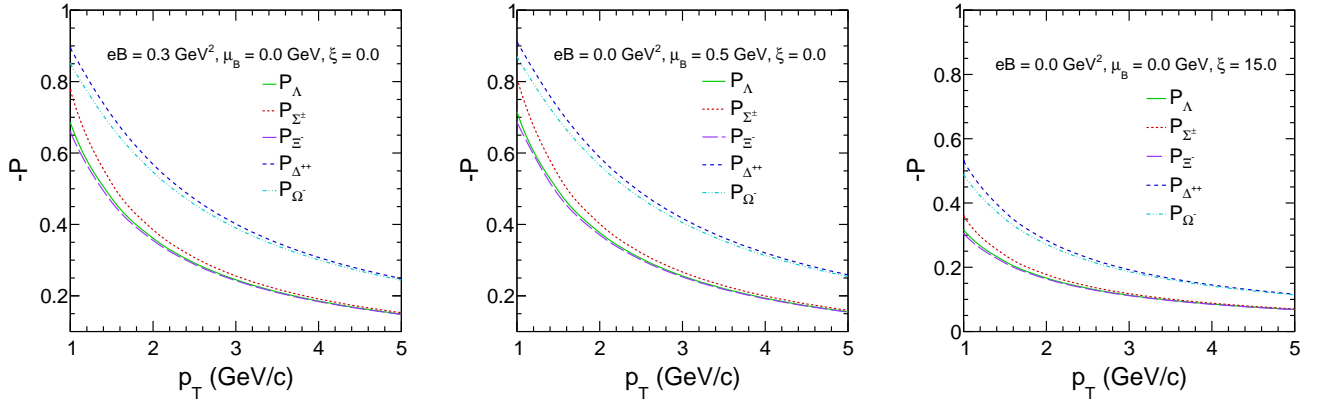


FIG. 4: (Color online)The variation of baryon polarization as a function of transverse momentum in the recombination process due to magnetic field (eB)(left panel), baryon chemical potential (μ_B)(middle panel) and anisotropic parameter (ξ)(right panel) at temperature $T = 200$ MeV.

of Λ hyperons aligns with the polarization of the initial strange quark. The initial strange quarks with lower momentum have higher values of Λ polarization after recombining to Λ hyperons and vice-versa. The middle panel of Fig. 2 illustrates the dependence of Λ hyperon polarization as a function of p_T for various values of chemical potential in the recombination scenario of hadronization. Three finite values of chemical potential are considered with $\mu_B = 0.1, 0.3,$ and 0.5 GeV. It can be seen here that there is no notable effect of baryon chemical potential on the polarization of Λ . The right panel of Fig. 2 depicts the variation of Λ polarization as a function of p_T for various values of the anisotropic parameter. Anisotropy in the medium is believed to restrict the alignment of particle spins along a specific

direction. Here, we considered four different values of anisotropic parameters, i.e., $\xi = 0.5, 1.0, 5.0, 15.0$, along with the isotropic case, i.e., $\xi = 0$. It is observed that the Λ hyperon polarization decreases with the anisotropy parameter. It is an intriguing observation that the medium anisotropy plays a significant role in influencing the polarization of Λ hyperons.

Figure 3 depicts the change in the Λ polarization with p_T corresponding to the fragmentation process of hadronization. The polarization of $\Lambda, \Sigma^\pm, \Xi^-, \Delta^{++},$ and Ω^- hyperons due to fragmentation is obtained using Eqs. 5, 6. The polarization corresponding to the fragmentation process is obtained using the n_s and f_s parameters. The values of these parameters

are extracted from Ref. [83]. Similar to Fig. 2, the polarization is shown for the same values of eB (left panel), μ_B (middle panel), and ξ (right panel) in Fig. 3. The p_T dependence of Λ hyperon polarization in the presence of an external magnetic field, baryon chemical potential, and medium anisotropy in the fragmentation process follow the same trend as the recombination process, except a change in the slope is observed at low p_T . However, the magnitude of Λ polarization due to fragmentation is comparably less than the recombination process.

Further, in Fig. 4, the variation in the polarization because of recombination is shown as a function of p_T at $eB = 0.3 \text{ GeV}^2$, $\mu_B = 0 \text{ GeV}$ and $\xi = 0$ for Λ , Σ^\pm , Ξ^- , Δ^{++} , and Ω^- hyperons. Moreover, we observe that the hyperon spin-polarization is dominant at low p_T . The middle and right panel of Fig. 4 shows Λ , Σ^\pm , Ξ^- , Δ^{++} , and Ω^- polarization with p_T for baryon chemical potential $\mu_B = 0.5 \text{ GeV}$ and anisotropic parameter $\xi = 15$, respectively. The role of baryon chemical potential on particle polarization is quite similar to the magnetic field. Fig. 4 indicates a quark flavor-dependent polarization of hyperons in the heavy-ion collisions. We found that there is grouping among the particles of baryon octet with spin-1/2 and baryon decouplet with spin-3/2 during the spin-orbit coupling. Particles having the same quark flavor, for example, Ω^- (sss) and Δ^{++} (uuu) have similar spin-orientation along the direction of OAM as compared to particles having mixed quark flavor, e.g., Λ (uds), Σ^\pm (uus/dds), and Ξ^- (dss). Therefore, particles of the same species possibly have some correlation among themselves, which drives the spin polarization. This correlation might be absent in mixed species particles; such an observation is recently reported for ϕ meson in Ref. [49]. In addition, the baryon-decouplet of spin-3/2 has higher polarization as compared to the baryon-octet of spin-1/2. Therefore, particle spin might play a role in its polarization. However, to confirm the importance of spin in the global polarization picture and to better understand the polarization mechanism in heavy-ion collisions, the experimental verification of global polarization for different particles with different spin and/or magnetic moments is required. Although the recent measurement global polarization of Ξ and Ω hyperons at STAR hint at a possible hierarchy in the global polarization, i.e., $P_\Lambda < P_\Xi < P_\Omega$ [36]. The large systematic and statistical uncertainties raise a question as to whether the difference is either due to the mass, lifetime, strangeness quantum number, differential freeze-out, etc.

Similarly, Fig. 5 shows the dependence of Λ , Σ^\pm , Ξ^- , Δ^{++} , and Ω^- hyperon polarization as a function of p_T in the presence of external magnetic field (left panel), baryon chemical potential (middle panel) and medium anisotropy parameters (right panel) in the fragmentation process of hadronization. In the fragmentation process, the polarization of Δ^{++} and Ω^-

is 1/3 of the polarization due to the u and s quarks, respectively. Therefore, baryons having the same quark flavor, each quark contributes equally to the final state baryon polarization. Meanwhile, baryons of mixed quark flavors have linear combinations due to each flavor. As consequence, a significant decrease in the Δ^{++} , and Ω^- polarization is observed compared to Λ , Σ^\pm , and Ξ^- in Fig 5. However, the polarization in the fragmentation process is always less compared to recombination for all baryons. The change in the polarization due to fragmentation in the presence of the magnetic field, baryon chemical potential, and medium anisotropy follow the same trend of the polarization obtained from the recombination process.

The left panel of Fig. 6 shows the combined effect of the magnetic field, baryon chemical potential, and medium anisotropy on Λ hyperon polarization. The interplay of these three effects is examined in Fig 6. We found that the medium anisotropy has a prevalent impact on the polarization observable as compared to the magnetic field and baryon chemical potential. The observed feature of medium anisotropy on polarization is due to the influence of anisotropy on Debye mass. Medium anisotropy plays a crucial role in controlling the spin-polarization of hyperon, which needs an extensive investigation from a theoretical standpoint. The right panel of Fig. 6 shows change in the polarization for Λ along with Σ^\pm , Ξ^- , Ω^- , and Δ^{++} baryons corresponding to the combined effect of the magnetic field, baryon chemical potential, and medium momentum-space anisotropy.

B. Spin alignment of vector mesons

Similar to the global polarization of hyperon, the spin-alignment of vector meson is also based on the same mechanism of spin-orbit coupling. Since a vector meson with spin one can have three different spin orientations, the probability for its spin to align in a given direction is 1/3. Any value of the spin alignment differs from 1/3, which means the polarization of the vector meson is along that direction. With the recent large spin alignment measurement of ϕ vector meson at RHIC [41, 42] and LHC [44], it becomes a challenging and active area of research for the theoretical community to know the possible sources of spin alignment for ϕ vector meson. The spin alignment of vector meson comes from both constituent quark and anti-quark and hence its polarization is quadratic in vorticity [56].

The left panel of Fig. 7 shows the effect of magnetic field on the spin alignment of ϕ meson for two different hadronization scenarios as described in formalism section II. The curves below line 1/3 depict the spin alignment of ϕ -meson due to the recombination of polarized

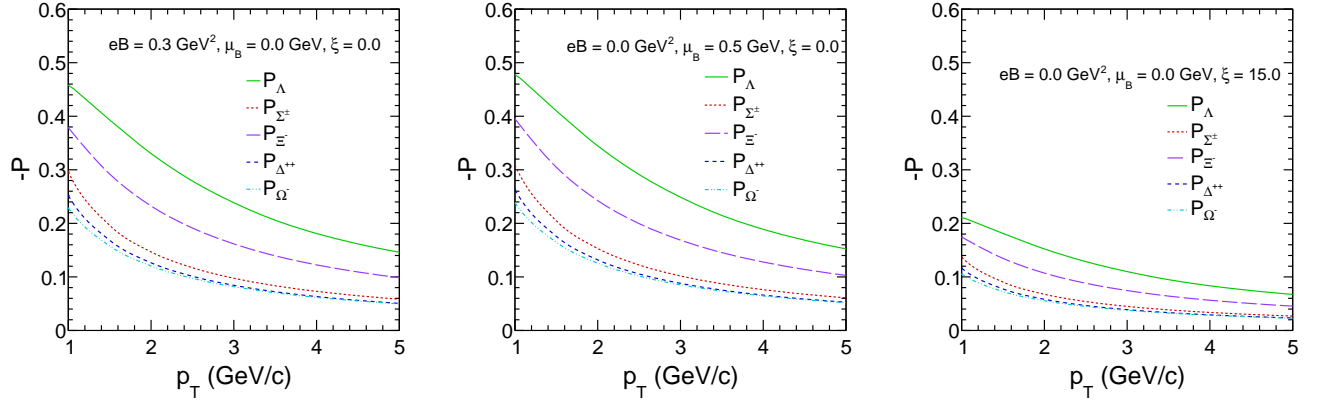


FIG. 5: (Color online) The variation of hyperon polarization as a function of transverse momentum due to the fragmentation process in the presence of magnetic field (eB)(left panel), baryon chemical potential (μ_B)(middle panel) and anisotropic parameter (ξ)(right panel) at temperature $T = 200$ MeV.

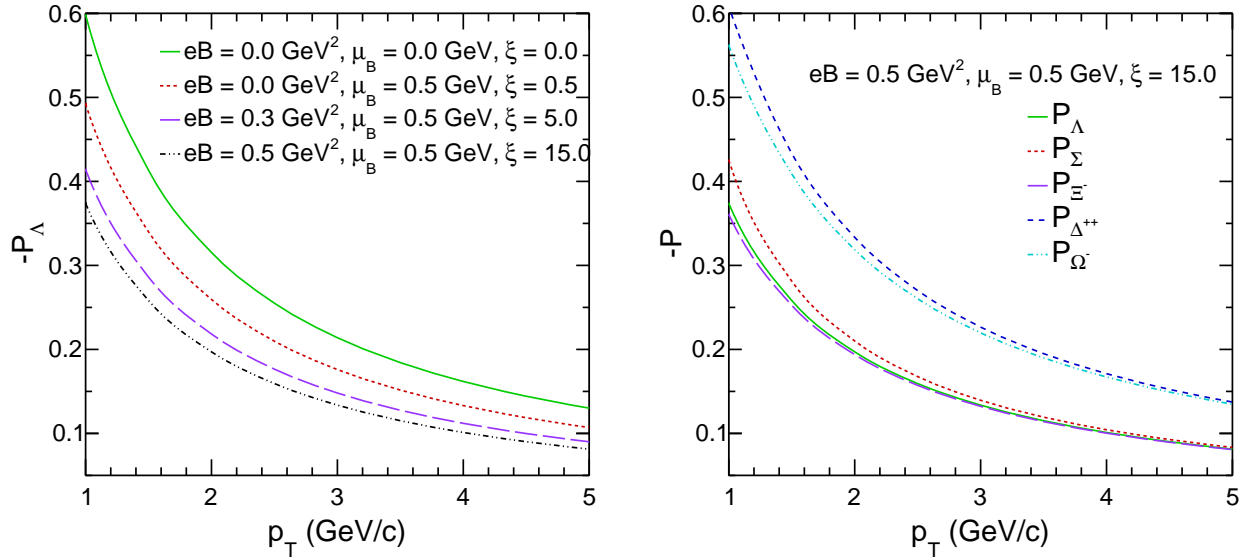


FIG. 6: (Color online) The variation of hyperon polarization as a function of transverse momentum due to magnetic field (left panel), baryon chemical potential (middle panel), and anisotropic parameter (right panel) at temperature $T = 200$ MeV.

quarks and anti-quarks. The curves above line 1/3 show the hadronization process of quark and anti-quark pairs in which either of them is created in the fragmentation process. We compare the obtained results with the STAR Collaboration data for Au+Au collisions for various centers of mass energies in (20-60)% bin [41]. The choice of center of mass energy selection of STAR data for Au+Au collisions in Fig 7 and Fig. 8 is just for illustration pur-

poses, and it has nothing specific relation with the magnetic field and anisotropy. It is found that the absolute deviation of ρ_{00} from 1/3 ($|\rho_{00} - 1/3|$) for ϕ vector meson increases with magnetic field for both cases of hadronization processes. The magnetic field aligns the particle spin in a specific direction; hence, it helps to enhance the degree of spin alignment. It is evident that the spin alignment of vector meson is directly proportional to

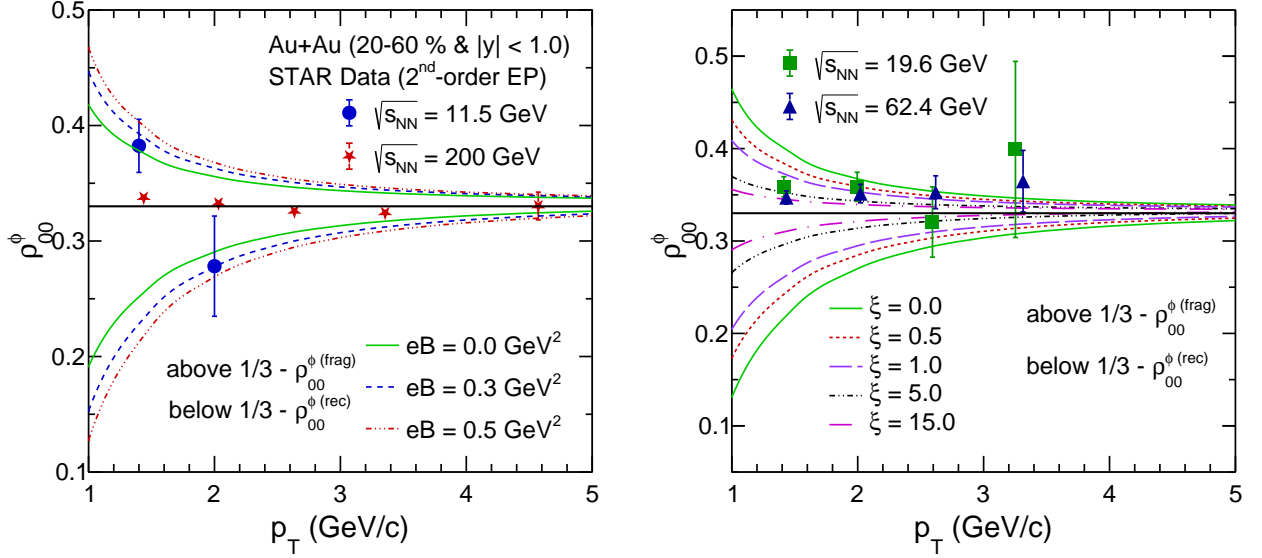


FIG. 7: (Color online) The variation of spin alignment of ϕ vector meson as a function of transverse momentum due to the magnetic field (left panel) and anisotropic parameter (right panel) at temperature $T = 200$ MeV. The results are compared with STAR measurements taken from Ref. [41].

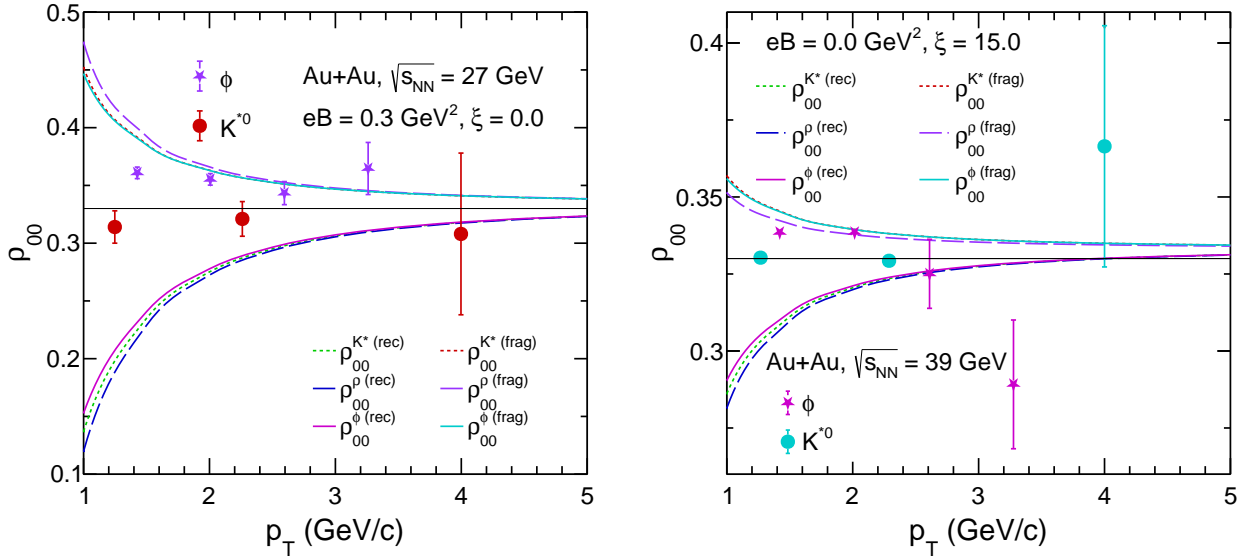


FIG. 8: (Color online) The variation of spin alignment of ϕ , K^{*0} , ρ vector meson as a function of transverse momentum due to the magnetic field (left panel), and anisotropic parameter (right panel) at temperature $T = 200$ MeV. The results are compared with STAR measurements taken from Ref. [41].

the square of the magnetic field. Since baryon chemical potential does not have a substantial effect on hyperon polarization, we have neglected the effect of baryon chemical potential on the spin alignment measurement of vector meson. The right panel of Fig. 7 shows the effect of ξ on the spin alignment of ϕ meson with a set of ξ values. From the figure, it is evident that medium anisotropy significantly modifies the vector meson spin alignment. The left panel of Fig. 8 shows the spin alignment of ϕ , K^* , and ρ meson at $eB = 0.5 \text{ GeV}^2$ for corresponding to fragmentation and recombination hadronization scenarios. The right panel of Fig. 8 shows the spin alignment of ϕ , K^* , and ρ meson for $\xi = 15$. Figure 7 and 8 depicts the absolute deviation of ρ_{00} from $1/3$ is more at low p_T for the recombination process as compared to the fragmentation. This implies that the degree of spin alignment is more at low p_T in the recombination process for ϕ , K^* , and ρ vector mesons. The value of ρ_{00} is close to $1/3$ towards high p_T showing zero spin alignment for ϕ , K^* , and ρ mesons. In the quark polarization model, the polarization of a quark is inversely proportional to the square of its mass, which suggests a mass ordering in the spin alignment effect of vector mesons due to their constituent quark composition. Figure 8 depicts $\rho_{00}^\rho > \rho_{00}^{K^*} > \rho_{00}^\phi$ at low p_T in the recombination scenario.

IV. CONCLUSION

In summary, we explored the global polarization of hyperons and spin-alignment of vector mesons in the presence of magnetic field, baryon chemical potential, and medium momentum-space anisotropy. The individual and combined effect of these parameters on hyperons and vector mesons polarization have been studied in the recombination and fragmentation process of hadronization. We found that the polarization of hyperons and spin-alignment of vector mesons increases with the increase in magnetic field. In this study, the baryon chemical potential has negligible dependence on hyperon polarization. The medium anisotropy significantly affects the polarization and spin alignment of

hadrons. It is interesting to note that the recombination process dominates at low p_T in comparison with the fragmentation process. The Debye mass-based polarization may have a substantial implication on particle production yield. Therefore, for a comprehensive study, one may include such an effect to study the hadron production in heavy-ion collisions.

The hyperon polarization obtained through the global quark polarization method is comparably higher than the experimentally measured hyperon polarization in heavy-ion collisions at RHIC. In addition to the magnetic field, baryon chemical potential, and medium momentum-space anisotropy used in this work, there may be various other sources that may affect the hyperon polarization. Such sources could be medium rotation, hadronic interactions, anisotropic flows in the medium, and fluctuation of other force fields such as vorticity, temperature gradient, shear tensor, strong force field, etc. However, the contribution of these sources on hyperon polarization has yet to be studied collectively. The qualitative prediction of global polarization is an open challenge and requires further investigation.

ACKNOWLEDGEMENT

Bhagyarathi Sahoo acknowledges the financial aid from CSIR, Government of India. The authors gratefully acknowledge the DAE-DST, Government of India funding under the mega-science project "Indian Participation in the ALICE experiment at CERN" bearing Project No.SR/MF/PS-02/2021-IITI (E-37123).

-
- [1] J. Adam *et al.* [ALICE Collaboration], *Nature Phys.* **13**, 535 (2017).
 - [2] V. Khachatryan *et al.* [CMS Collaboration], *Phys. Lett. B* **765**, 193 (2017).
 - [3] A. Ortiz Velasquez, P. Christiansen, E. Cuautle Flores, I. Maldonado Cervantes and G. Paić, *Phys. Rev. Lett.* **111**, 042001 (2013).
 - [4] C. Zhang, A. Behera, S. Bhatta and J. Jia, *Phys. Lett. B* **822**, 136702 (2021).
 - [5] B. Sahoo, D. Sahu, S. Deb, C. R. Singh and R. Sahoo, [arXiv:2308.15151 [hep-ph]].
 - [6] K. Fukushima, D. E. Kharzeev and H. J. Warringa, *Phys. Rev. D* **78**, 074033 (2008).
 - [7] D. E. Kharzeev, L. D. McLerran and H. J. Warringa, *Nucl. Phys. A* **803** 227 (2008).
 - [8] O. Rogachevsky, A. Sorin and O. Teryaev, *Phys. Rev. C* **82**, 054910 (2010).
 - [9] D. Kharzeev and A. Zhitnitsky, *Nucl. Phys. A* **797**, 67 (2007).
 - [10] F. Becattini and I. Karpenko, *Phys. Rev. Lett.* **120**, 012302 (2018).
 - [11] J. Adam *et al.* [STAR Collaboration], *Phys. Rev. Lett.* **123**, 132301 (2019).

- [12] Z. T. Liang and X. N. Wang, Phys. Rev. Lett. **94**, 102301 (2005). [erratum: Phys. Rev. Lett. **96** (2006), 039901]
- [13] Z. T. Liang and X. N. Wang, Phys. Lett. B **629**, 20 (2005).
- [14] Z. t. Liang, J. Phys. G **34**, S323-330 (2007).
- [15] J. H. Gao, S. W. Chen, W. t. Deng, Z. T. Liang, Q. Wang and X. N. Wang, Phys. Rev. C **77**, 044902 (2008).
- [16] D. L. Adams *et al.* [FNAL-E704], Phys. Lett. B **264**, 462(1991).
- [17] A. Ipp, A. Di Piazza, J. Evers and C. H. Keitel, Phys. Lett. B **666**, 315 (2008).
- [18] F. Becattini, V. Chandra, L. Del Zanna and E. Grossi, Annals Phys. **338** 32 (2013).
- [19] B. I. Abelev *et al.* [STAR Collaboration], Phys. Rev. C **76**, 024915 (2007).
- [20] L. Adamczyk *et al.* [STAR Collaboration], Nature **548** 62 (2017).
- [21] J. Adam *et al.* [STAR Collaboration], Phys. Rev. C **98**, 014910 (2018).
- [22] S. Alzhrani, S. Ryu and C. Shen, Phys. Rev. C **106**, 014905 (2022).
- [23] O. Vitiuk, L. V. Bravina and E. E. Zabrodin, Phys. Lett. B **803**, 135298 (2020).
- [24] Y. Jiang, Z. W. Lin and J. Liao, Phys. Rev. C **94** (2016) no.4, 044910 [erratum: Phys. Rev. C **95** (2017) no.4, 049904]
- [25] Y. Sun and C. M. Ko, Phys. Rev. C **96**, 024906 (2017).
- [26] Y. B. Ivanov, V. D. Toneev and A. A. Soldatov, Phys. Rev. C **100**, 014908 (2019).
- [27] K. K. Pradhan, B. Sahoo, D. Sahu and R. Sahoo, [arXiv:2304.05190 [hep-ph]].
- [28] L. P. Csernai, V. K. Magas and D. J. Wang, Phys. Rev. C **87**, 034906 (2013).
- [29] L. P. Csernai, D. J. Wang, M. Bleicher and H. Stöcker, Phys. Rev. C **90**, 021904 (2014).
- [30] L. G. Pang, H. Petersen, Q. Wang and X. N. Wang, Phys. Rev. Lett. **117**, 192301 (2016).
- [31] H. Li, L. G. Pang, Q. Wang and X. L. Xia, Phys. Rev. C **96**, 054908 (2017).
- [32] B. Fu, K. Xu, X. G. Huang and H. Song, Phys. Rev. C **103**, 024903 (2021).
- [33] I. Karpenko and F. Becattini, Nucl. Phys. A **967**, 764 (2017).
- [34] F. Becattini and M. A. Lisa, Ann. Rev. Nucl. Part. Sci. **70**, 395 (2020).
- [35] Xie, Y., Wang, D. and Csernai, L.P., Eur. Phys. J. C **80**, 39 (2020).
- [36] J. Adam *et al.* [STAR Collaboration], Phys. Rev. Lett. **126**, 162301 (2021).
- [37] S. Acharya *et al.*, [ALICE Collaboration], Phys. Lett. B **815**, 136146 (2021).
- [38] S. Acharya *et al.*, [ALICE Collaboration], Phys. Rev. Lett. **131**, 042303 (2023).
- [39] L. Adamczyk *et al.*, [STAR Collaboration], Phys. Lett. B **739**, 180 (2014).
- [40] J. Adam *et al.*, [STAR Collaboration], Phys. Rev. D **102**, 092009 (2020).
- [41] M. S. Abdallah *et al.* [STAR Collaboration], Nature **614** 244 (2023).
- [42] S. Singha [STAR Collaboration], Nucl. Phys. A **1005**, 121733 (2021).
- [43] B. I. Abelev *et al.* [STAR Collaboration], Phys. Rev. C **77**, 061902 (2008).
- [44] S. Acharya *et al.* [ALICE Collaboration], Phys. Rev. Lett. **125**, 012301 (2020).
- [45] R. Singh [ALICE Collaboration], Nucl. Phys. A **982**, 515 (2019).
- [46] B. Mohanty, S. Kundu, S. Singha and R. Singh, Mod. Phys. Lett. A **36**, 2130026 (2021).
- [47] L. P. Csernai, J. I. Kapusta and T. Welle, Phys. Rev. C **99**, 021901 (2019).
- [48] X. L. Sheng, L. Oliva and Q. Wang, Phys. Rev. D **101**, 096005 (2020). [erratum: Phys. Rev. D **105**, 099903 (2022).]
- [49] X. L. Sheng, L. Oliva, Z. T. Liang, Q. Wang and X. N. Wang, Phys. Rev. Lett. **131**, 042304 (2023).
- [50] F. Becattini, M. Buzzegoli, G. Inghirami, I. Karpenko and A. Palermo, Phys. Rev. Lett. **127**, 272302 (2021).
- [51] H. Z. Wu, L. G. Pang, X. G. Huang and Q. Wang, Phys. Rev. Research. **1**, 033058 (2019).
- [52] X. L. Xia, H. Li, X. G. Huang and H. Zhong Huang, Phys. Lett. B **817** (2021), 136325
- [53] V. Skokov, A. Y. Illarionov and V. Toneev, Int. J. Mod. Phys. A **24**, 5925 (2009).
- [54] B. Sahoo, C. R. Singh, D. Sahu, R. Sahoo and J. e. Alam, Eur. Phys. J. C **83**, 873 (2023).
- [55] B. Sahoo, K. K. Pradhan, D. Sahu and R. Sahoo, Phys. Rev. D **108**, 074028 (2023).
- [56] Y. G. Yang, R. H. Fang, Q. Wang and X. N. Wang, Phys. Rev. C **97**, 034917 (2018).
- [57] X. L. Sheng, Q. Wang and X. N. Wang, Phys. Rev. D **102**, 056013 (2020).
- [58] F. Becattini, I. Karpenko, M. Lisa, I. Upsal and S. Voloshin, Phys. Rev. C **95**, 054902 (2017).
- [59] S. Wu and Y. Xie, Eur. Phys. J. A **59**, 108 (2023).
- [60] Z. Z. Han and J. Xu, Phys. Lett. B **786**, 255 (2018).
- [61] K. Xu, F. Lin, A. Huang and M. Huang, Phys. Rev. D **106**, L071502 (2022).
- [62] A. Ayala, M. A. Ayala Torres, E. Cuautle, I. Domínguez, M. A. Fontaine Sanchez, I. Maldonado, E. Moreno-Barbosa, P. A. Nieto-Marín, M. Rodríguez-Cahuantzi and J. Salinas, *et al.* Phys. Lett. B **810**, 135818 (2020).
- [63] X. Guo, J. Liao and E. Wang, Sci. Rep. **10**, 2196 (2020).
- [64] J. H. Gao, Z. T. Liang, S. Pu, Q. Wang and X. N. Wang, Phys. Rev. Lett. **109**, 232301 (2012).
- [65] L. Dong, Y. Guo, A. Islam and M. Strickland, Phys. Rev. D **104**, 096017 (2021).
- [66] B. Karmakar, A. Bandyopadhyay, N. Haque and M. G. Mustafa, Eur. Phys. J. C **79**, 658 (2019).
- [67] H. X. Zhang, J. W. Kang and B. W. Zhang, Eur. Phys. J. C **81**, 623 (2021).
- [68] A. Bandyopadhyay, B. Karmakar, N. Haque and M. G. Mustafa, Phys. Rev. D **100**, 034031 (2019).
- [69] B. Singh, L. Thakur and H. Mishra, Phys. Rev. D **97**, 096011 (2018).
- [70] N. Haque, A. Bandyopadhyay, J. O. Andersen, M. G. Mustafa, M. Strickland and N. Su, JHEP **05**, 027 (2014).
- [71] J. Zhao and B. Chen, Phys. Rev. C **107**, 044909 (2023).
- [72] D. Lafferty and A. Rothkopf, Phys. Rev. D **101**, 056010 (2020).
- [73] G. Huang and P. Zhuang, Phys. Rev. D **104**, 074001 (2021).
- [74] M. Le Bellac, Thermal Field Theory (Cambridge University Press, Cambridge, England, 1996).
- [75] L. Dong, Y. Guo, A. Islam, A. Rothkopf and M. Strickland, JHEP **09**, 200 (2022).

- [76] M. Strickland and D. Bazow, Nucl. Phys. A **879**, 25-58 (2012).
- [77] P. Romatschke and M. Strickland, Phys. Rev. D **68**, 036004 (2003).
- [78] P. Romatschke and M. Strickland, Phys. Rev. D **70**, 116006 (2004).
- [79] M. Strickland, Anisotropic hydrodynamics: Three lectures, Acta Phys. Pol. B 45, 2355 (2014).
- [80] C. Bonati, M. D'Elia, M. Mariti, M. Mesiti, F. Negro, A. Rucci and F. Sanfilippo, Phys. Rev. D **95**, 074515 (2017).
- [81] A. Bandyopadhyay, C. A. Islam and M. G. Mustafa, Phys. Rev. D **94**, 114034 (2016).
- [82] A. Bandyopadhyay, R. L. S. Farias, B. S. Lopes and R. O. Ramos, Phys. Rev. D **100**, 076021 (2019).
- [83] J. w. Zhang, H. h. Li, F. l. Shao and J. Song, Chin. Phys. C **44**, 014101 (2020).